Electronic Supplementary Information (ESI)

Highly stable nanoporous covalent triazine-based frameworks with an adamantane core for carbon dioxide sorption and separation

Asamanjoy Bhunia,[a] Ishtvan Boldog,[a] Andreas Möller[b] and Christoph Janiak*[a]

[a] Institut für Anorganische Chemie und Strukturchemie, Heinrich-Heine-Universität Düsseldorf, 40204 Düsseldorf, Germany
[b] Institut für Nichtklassische Chemie e.V., Permoserstr. 15, D-04318 Leipzig, Germany.
* Corresponding author: E-mail: janiak@uni-duesseldorf.de; Fax: + 49-211-81-12287; Tel: +49-211-81-12286.

Supporting information
18 pages

Table of contents

1. Experimental Section

Materials and methods

All chemicals were purchased from commercial suppliers (Sigma-Aldrich, Acros Organics, and Alfa Aesar chemical company) and used without further purification, unless stated otherwise. 1,3-di(4-cyanophenyl)adamantane, 1,3,5-tri(4-cyanophenyl)adamantane and 1,3,5,7-tetrakis(4-cyano-phenyl)adamantane were synthesized according to the reported procedures (see below).[1,2] Chloroform was distilled from P_2O_5 under a nitrogen atmosphere.

Infrared (IR) spectra were obtained on a Bruker FT-IR Tensor 37 Spectrometer in the 4000-550 cm^{-1} region with 2 cm^{-1} resolution as KBr disks. ^{1}H and ^{13}C spectra were recorded on a Avance DRX-500 instruments. ^{1}H and ^{13}C NMR chemical shifts are given in ppm relative to $SiMe_4$ (δ = 0.0 ppm) with calibration against the (residual protonated) solvent signal ($CDCl_3$: 7.26 (^{1}H) and 77.0 (^{13}C)). Elemental (CNH) analyses were carried out with a PerkinElmer 2400 series 2 elemental analyzer. Powder X-ray diffraction (PXRD) data was collected on a Bruker D2 Phaser diffractometer using a flat sample holder (also a flat silicon, low background sample holder) and Cu $K\alpha_1/\alpha_2$ radiation with λ = 1.5418 Å at 30 kV covering 2theta angles 5-80° over a time of 2 h, that is. 0.01°/sec. Diffractograms were obtained on flat layer sample holders where at low angle the beam spot is strongly broadened so that only a fraction of the reflected radiation reaches the detector, which leads to low relative intensities measured at $2\theta < 7°$. For hygroscopic or air-sensitive samples, the sample holder can be sealed with a dome. Scanning electron microscopy (SEM) images were obtained using an ESEM Quanta 400 FEG SEM equipped with a secondary electron detector. Thermogravimetric analyses (TGA) were carried out at a ramp rate of 5 °C/min in a N_2 flow with a Netzsch Thermo-Microbalance Aparatus TG 209 F3 Tarsus.

Sorption isotherms were measured using a Micromeritics ASAP 2020 automatic gas sorption analyzer equipped with oil-free vacuum pumps (ultimate vacuum $<10^{-8}$ mbar) and valves, which guaranteed contamination free measurements. The sample was connected to the preparation port of the sorption analyzer and degassed under vacuum until the outgassing rate, i.e., the rate of pressure rise in the temporarily closed manifold with the connected sample tube, was less than 2 μTorr/min at the specified temperature 200 °C. After weighing, the sample tube was then transferred to the analysis port of the sorption analyzer. All used gases (H_2, He, N_2, CO_2, CH_4) were of ultra high purity (UHP, grade 5.0, 99.999%) and the STP volumes are given according to the NIST standards (293.15 K, 101.325 kPa). Helium gas was used for the determination of the cold and warm free space of the sample tubes. H_2 and N_2 sorption isotherms were measured at 77 K (liquid nitrogen bath), whereas CO_2 and CH_4 sorption isotherms were measured at 293±1 K (passive thermostating)

and 273.15 K (ice/deionized water bath). The heat of adsorption values and the DFT pore size distributions ('N_2 DFT slit pore' model) were calculated out using the ASAP 2020 v3.05 software. Nitrogen sorption isotherms were also obtained on a Quantachrome Nova 4000e at 77 K.

Syntheses

1,3-bis(4-cyanophenyl)adamantane: The colorless compound was synthesized in 88% yield according to a previously reported two-step procedure[2] starting from 1,3-diphenyladamantane.[1] ^{1}H NMR ($CDCl_3$, 500MHz): δ = 7.55 (d, 4H, Ar), 7.41 (d, 4H, Ar), 2.31 (s, 2H, Ad), 1.92(m, 2H, Ad), 1.89(m, 8H, Ad), 1.74 (t, 2H, Ad). ^{13}C NMR ($CDCl_3$, 500MHz): δ = 156 (**C**$_{Ar}$H), 133 (**C**$_{Ar}$H), 126 (**C**$_{Ar}$H), 119 (**C**N), 110 (C$_{Ar}$H), 48 (**C**$_{Ad}$H$_2$), 42(**C**$_{Ad}$H$_2$), 38 (**C**$_{Ad}$H$_2$), 36 (**C**$_{Ad}$), 30 (C$_{ad}$H). IR (KBr pellet): ῡ = 3437 (br), 3092 (w), 3064 (w), 2900 (s), 2848 (m), 2226 (s), 1655 (w), 1604 (s), 1521 (w), 1503 (s), 1407 (m), 1345 (w), 1322 (m), 1287 (w), 1265 (m), 1244 (w), 1177 (m), 1113 (w), 1015 (m), 954 (w), 854 (w), 821 (s), 775 (w), 737 (w), 675 (w), 562 (s), 521 (w), cm^{-1}

1,3,5-tris(4-cyanophenyl)adamantane: The colorless compound was synthesized in 87% yield according to a previously reported two-step procedure[2] starting from 1,3,5-triphenyladamantane.[1,3] ^{1}H NMR ($CDCl_3$, 500MHz): δ= 7.64 (d, 6H, Ar), 7.54 (d, 6H, Ar), 2.64 (sep, 1H, Ad), 2.10-2.03 (m, 12, Ad). ^{13}C NMR ($CDCl_3$, 500MHz): δ = 154 (**C**$_{Ar}$H), 132 (**C**$_{Ar}$H), 126 (**C**$_{Ar}$H), 119 (**C**N), 110 (C$_{Ar}$H), 47 (**C**$_{Ad}$H$_2$),, 41 (**C**$_{Ad}$H$_2$), 39 (**C**$_{Ad}$), 30 (**C**$_{Ad}$H$_2$). IR (KBr pellet): ῡ = 3435 (br), 3070 (w), 3042 (w), 2928 (m), 2906 (m), 2855 (m), 2358 (w), 2226 (s), 1635 (w), 1605 (s), 1559 (w), 1505 (s), 1449 (m), 1402 (m), 1360 (w), 1342 (w), 1253 (w), 1176 (m), 1116 (w), 1017 (m), 980 (w), 869 (m), 831 (s), 785 (w), 737 (w), 600 (w), 572 (s), 531 (w), 459 (w), 420 (w) cm^{-1}

1,3,5,7-tetrakis(4-cyanophenyl)adamantane: The colorless compound was synthesized in 82% yield according to a previously reported two-step procedure[2] starting from 1,3,5,7-triphenyladamantane.[1]
^{1}H NMR (DMSO-D$_6$, 500MHz): δ= 2.12 (s, 12H); 7.80 (broad s, 16H). ^{13}C NMR (DMSO-d$_6$, 500MHz): δ= 44.5 (**C**$_{Ad}$H$_2$), 109, 119, 127 (**C**$_{Ar}$H), 132 (C$_{Ar}$H). IR (KBr pellet): ῡ = 3435 (br), 3070 (w), 3042 (w), 2928 (m), 2906 (m), 2855 (m), 2358 (w), 2226 (s), 1632 (w), 1605 (s), 1562 (w), 1542 (w), 1525 (w), 1505 (s), 1453 (w), 1444 (w), 1404 (m), 1385 (w), 1361 (m), 1223 (w), 1195 (w), 1174 (w), 1117 (w), 1019 (m), 893 (w), 837 (s), 793 (m), 741 (w), 567 (s), 524 (w), 421 (w) cm^{-1}

PCTF-3: A mixture of 1,3-di(4-cyanophenyl)adamantane (102 mg, 0.3 mmol) and $ZnCl_2$ (408 mg, 3.0 mmol) were placed into a Pyrex ampoule under inert conditions. The ampoule was evacuated, sealed and heated to 400 °C for 48 h followed by cooling to room temperature. The black product was collected and stirred with water for 72 h. Then the product was isolated by filtration and again stirred with 100 mL of 2 mol/L HCl for 24 h. The resulting black powder was further washed with water (3 × 50 mL), THF (3 × 30 mL), acetone (3 × 30 mL) and dried in vacuum. Yield: 85 mg, 83 % for $(C_{66}H_{62}N_6)_n$.

PCTF-4: The procedure for PCTF-3 was followed by using the precursor compound 1,3,5-tri(4-cyanophenyl)adamantane (88 mg, 0.2 mmol) and $ZnCl_2$ (272 mg, 2.0 mmol). Yield: 74 mg, 84 % for $(C_{93}H_{75}N_9)_n$.

PCTF-5: The procedure for PCTF-3 was followed by using 1,3,5,7-tetrakis(4-cyanophenyl)adamantane (81 mg, 0.15 mmol) and $ZnCl_2$ (204 mg, 1.5 mmol). Yield: 72 mg, 89 % for $(C_{114}H_{84}N_{12})_n$.

PCTF-6: A 50 ml Schlenk flask was charged with trifluoromethanesulfonic acid (0.15 g, 1.0 mmol) in 10 mL dry $CHCl_3$ under N_2 atmosphere. The reaction mixture was stirred and cooled to 0 °C. Di-(4-cyanophenyl)adamantane (85 mg, 0.25 mmol) in 30 mL dry $CHCl_3$ was added dropwise into the acid solution with stirring over 30 min and the temperature of 0 °C was maintained for another 2 h. Then, the resulting solution was stirred for 12 h at room temperature. An NH_3/H_2O solution (0.5 mol/L) was added until the reaction mixture became neutral and the mixture was stirred for another 2 h. The light yellow product was isolated by filtration and washed with water (3 × 50 mL), THF (3 × 30 mL), acetone (3 × 30 mL) and chloroform (3 × 30 mL), and dried in vacuum. Yield: 70 mg, 82 % for $(C_{66}H_{62}N_6)_n$.

PCTF-7: The procedure for PCTF-6 was followed by using 1,3,5-tri-(4-cyanophenyl)-adamantane (88 mg, 0.2 mmol) with trifluoromethanesulfonic acid (0.15 g, 1.0 mmol). Yield: 71 mg, 81 % for $(C_{93}H_{75}N_9)_n$.

For the washing we followed the previously published procedure in S. Ren, M. J. Bojdys, R. Dawson, A. Laybourn, Y. Z. Khimyak, D. J. Adams and A. I. Cooper, *Adv. Mater.*, 2012, **24**, 2357-2361. Other publications on COF or CTF materials which describe similar washing procedures are

T. Ben, H. Ren, S. Ma, D. Cao, J. Lan, X. Jing, W. Wang, J. Xu, F.Deng, J. M. Simmons, S. Qiu and G. Zhu, *Angew. Chem. Int. Ed.*, 2009, **48**, 9457-9460; M. G. Rabbani and H. M. El-Kaderi, *Chem. Mater.*, 2012, **24**, 1511-1517.

Several articles on CTFs where $ZnCl_2$ was used also demonstrated that minor amounts of zinc are still present in the CTF materials after washing, which decrease the surface area slightly. This difficult to avoid aspect was already established and discussed by Kuhn, Antonietti and Thomas et al. [P. Kuhn, M. Antonietti and A. Thomas, *Angew.Chem. Int. Ed.*, 2008, **47**, 3450-3453; P. Kuhn, A. l. Forget, D. Su, A. Thomas and M. Antonietti, *J. Am. Chem. Soc.*, 2008, **130**, 13333-13337; P. Kuhn, A. Thomas and M. Antonietti, *Macromolecules*, 2009, **42**, 319-326.; M. J. Bojdys, J. Jeromenok, A. Thomas and M. Antonietti, *Adv. Mater.*, 2010, **22**, 2202-2205.].

Note on solid-state ^{13}C NMR:

Recently, we have published a contribution dealing with porous covalent triazine-based frameworks (PCTF-1 and -2) (A. Bhunia, V. Vasylyeva and C. Janiak, *Chem. Commun.*, 2013, **49**, 3961-3963). In this Communication, we already tried to measure the solid state MAS ^{13}C NMR spectrum. However, we were unable to obtain a meaningful spectrum because PCTFs are carbonaceous materials bearing resemblance to graphite or graphene. The black samples of PCTF-1 and PCTF-2 are most likely conductive. Since, PCTF-3 to -5 are also similar kind of materials, therefore, we are also unable to measure the solid state ^{1}H as well as ^{13}C NMR spectrum. Rapid rotation of a conductive sample in a magnetic field will lead to strong heating of the sample and rotor.
The MAS NMR operator already had an accident where a graphene-like sample had exploded in the rotor, destroying the rotor and parts of the probe head inside the NMR instrument and causing about 7000 EUR of damage.
We still tried to measure the PCTF-1 and -2 samples by rotating them slowly at about 2-3 kHz instead of the normal 20-30 kHz with 13C-one pulse-experiments with decoupling and waiting times of 10 and 40 sec. Consequently only a broad hump was seen from 100-160 ppm. Such a broad hump from 100 to 160 ppm without fine-structure resolution was also seen in the solid state NMR of graphite oxide, for example (L. B. Casabianca, M. A. Shaibat, W. W. Cai, S. Park, R. Piner, R. S. Ruoff, and Y. Ishii, *J. Am. Chem. Soc.*, 2010, **132**, 5672-5676), graphene nanosheets (X. Wang. Y. Hu, L. Song, H. Yang, W. Xing, H. Lu, *J. Mater. Chem.*, 2011, **21**, 4222-4227), hydrothermally (from graphite oxide) reduced graphene sheets (D. Long, W. Li, L. Ling, J. Miyawaki, I. Mochida, S.-H. Yoon, *Langmuir*, 2010, **26**, 16096-16102) or multi-walled carbon nanotubes (E. Abou-Hamad, M.-R. Babaa, M. Bouhrara, Y. Kim, Y. Saih, S. Dennler, F. Mauri, J.-M. Basset, C. Goze-Bac, and T. Wågberg, *Phys. Rev. B*, 2011, **84**, 165417)
Hence, similar to graphene no fine structure could be seen in the solid-state MAS ^{13}C NMR spectra of the PCTF samples.

2. FT-IR Spectrum

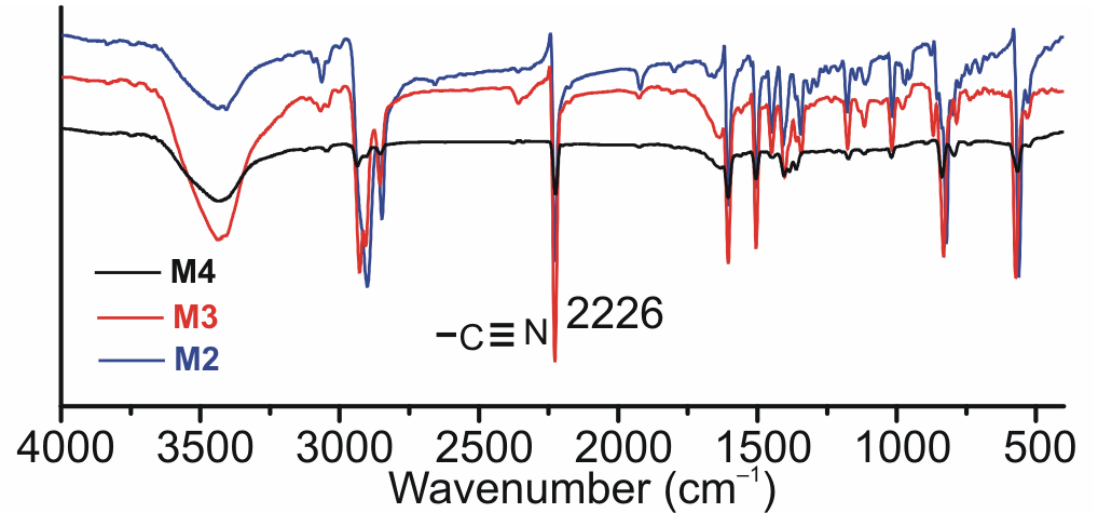

Fig. S1 IR spectra of monomers (M2-M4).

3. Powder X-ray diffraction patterns

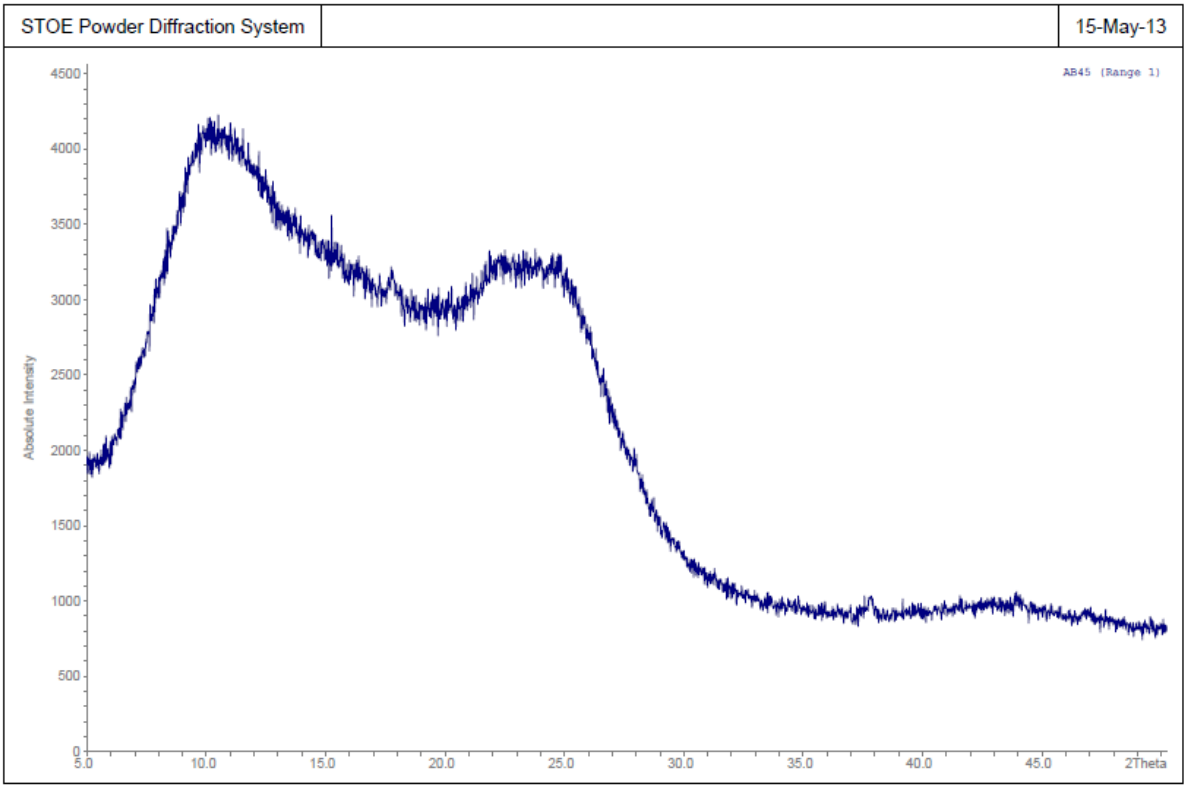

Fig. S2 Powder X-ray pattern of PCTF-3.

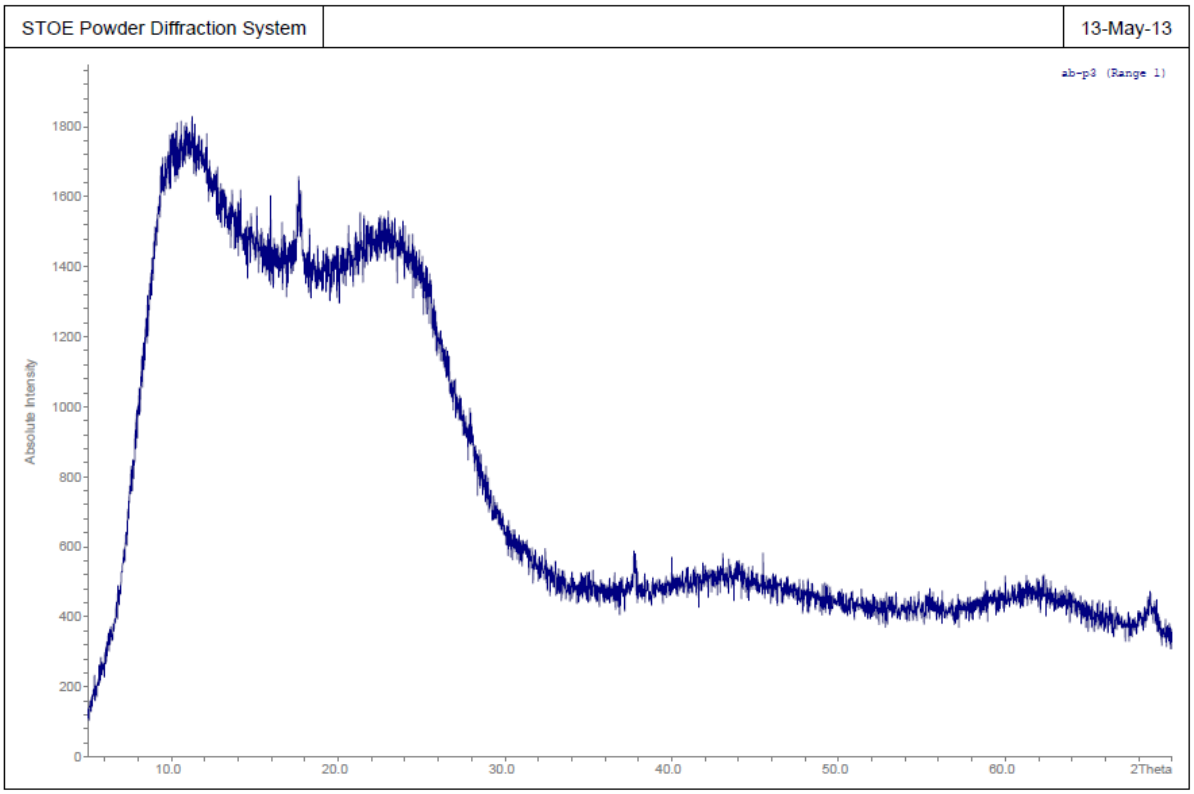

Fig. S3 Powder X-ray pattern of PCTF-4.

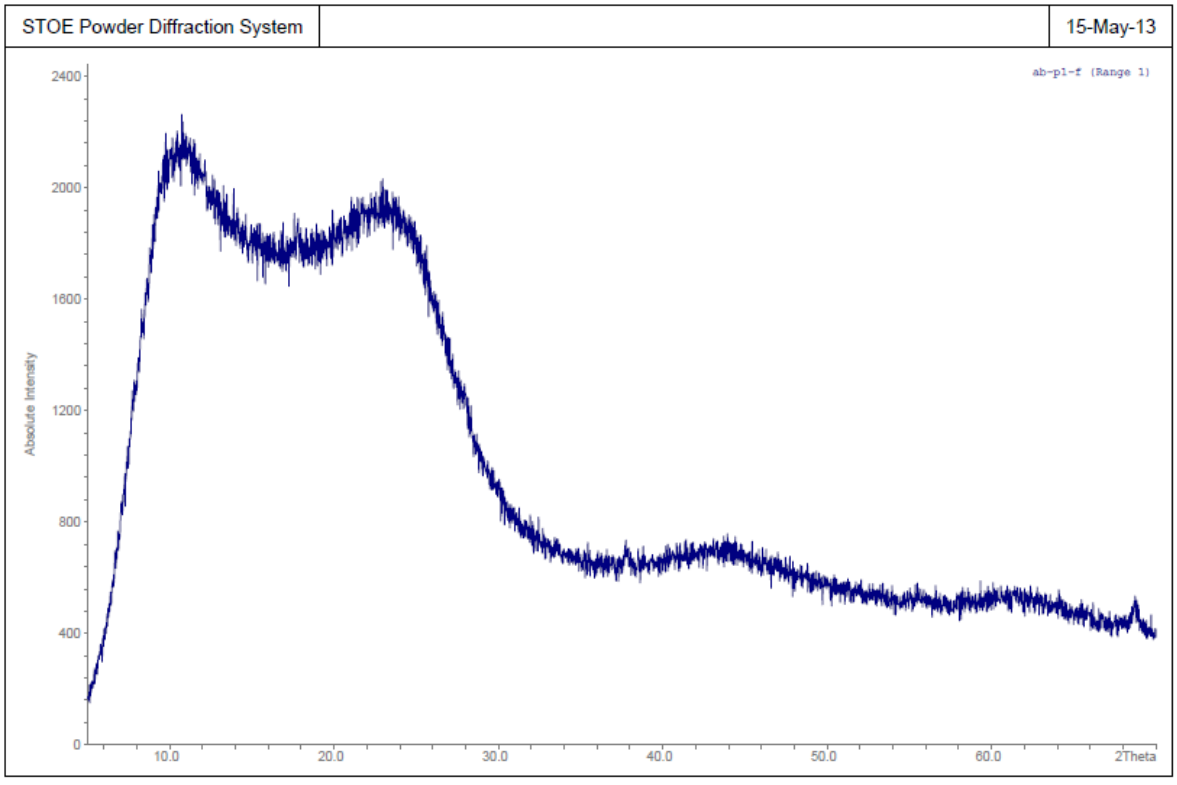

Fig. S4 Powder X-ray pattern of PCTF-5.

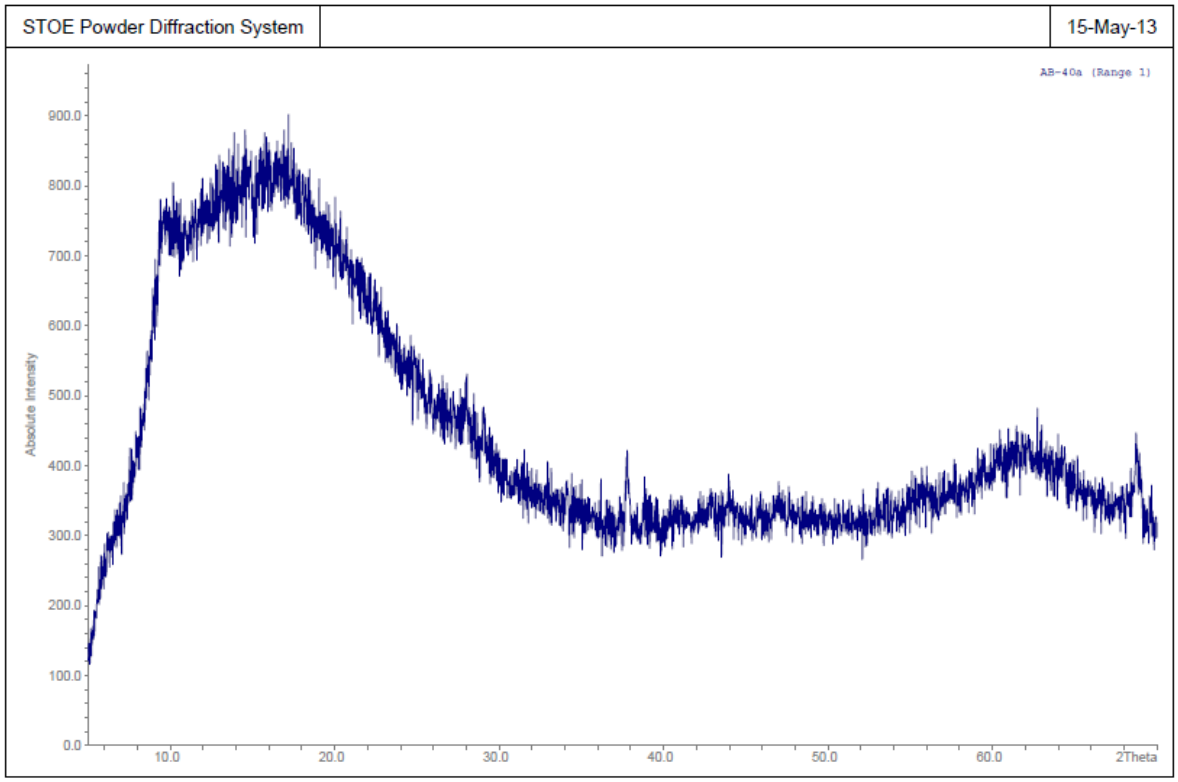

Fig. S5 Powder X-ray pattern of PCTF-6.

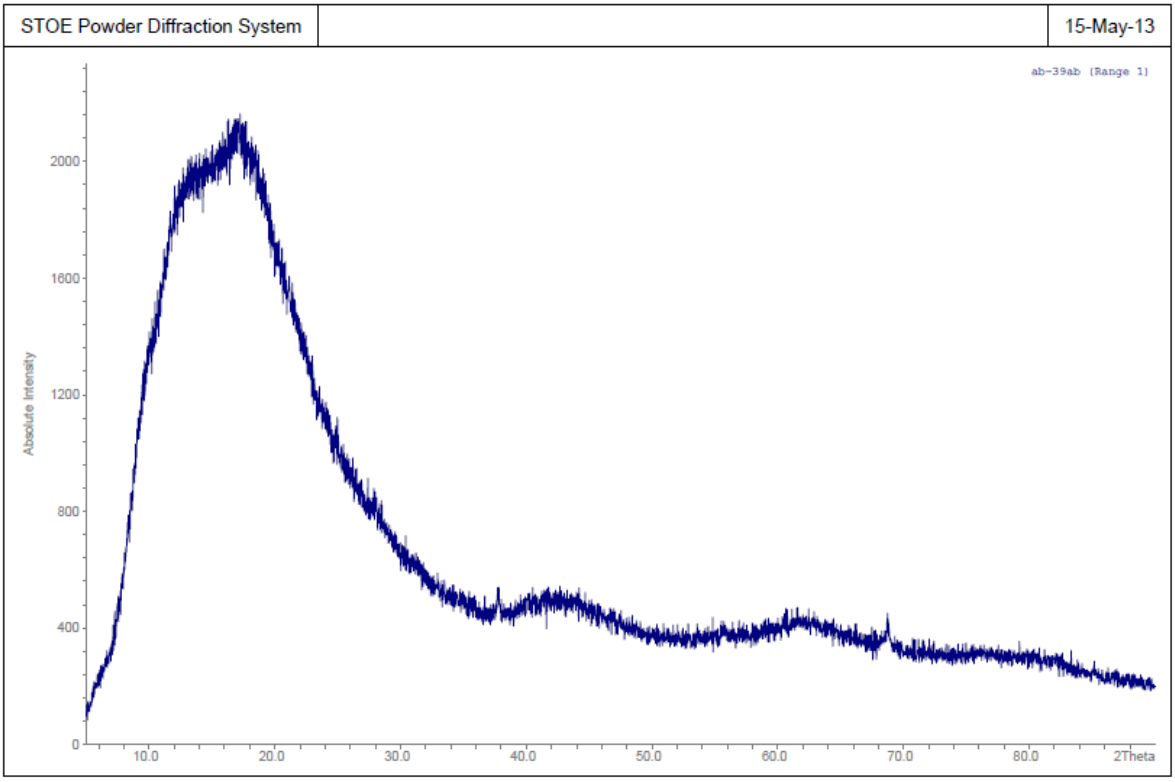

Fig. S6 Powder X-ray pattern of PCTF-7.

4. Elemental analysis of PCTFs

Table S1 Elemental analysis of PCTFs

Compounds	Calculated (%)[a]					Found (%)				
	C	H	N	C/H	C/N	C	H	N	C/H	C/N
PCTF-3	84.4	6.65	8.95	12.69	9.43	88.94	3.59	1.59	24.77	55.94
PCTF-4	84.71	5.73	9.56	14.78	8.86	87.1	3.36	2.08	25.92	41.87
PCTF-5	84.42	5.22	10.36	16.17	8.15	79.35	3.29	1.47	24.12	53.98
PCTF-6	84.4	6.65	8.95	12.69	9.43	66.94	4.74	5.20	14.12	12.87
PCTF-7	84.71	5.73	9.56	14.78	8.86	68.41	5.39	7.27	12.69	9.40

The elemental analysis of PCTF-3 to PCTF-5 give a much lower nitrogen content and concomitantly a much higher than calculated C/N ratio. This indicates that most of the nitrogen is lost to decomposition (Scheme S1).

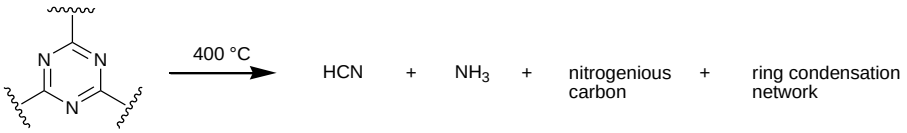

Scheme S1: General schematic representation for the decomposition of a triazine ring in, e.g., PCTFs.

In PCTF-6 and PCTF-7, the calculated and found C/H and C/N ratios are comparatively close.

5. Thermogravimetric analysis

All PCTFs (PCTF-3 to PCTF-7) show definite weight loss before decomposition. Both weight loss and decomposition temperature were summarized in Table S2.

Table S2 Decomposition temperature for PCTFs

Compound	Decomposition Temperature (°C)	Weight loss (%)
PCTF-3	460	7.38
PCTF-4	500	2.4
PCTF-5	500	5.11
PCTF-6	490	8.72
PCTF-7	490	8.55

6. Pore size distribution of PCTFs

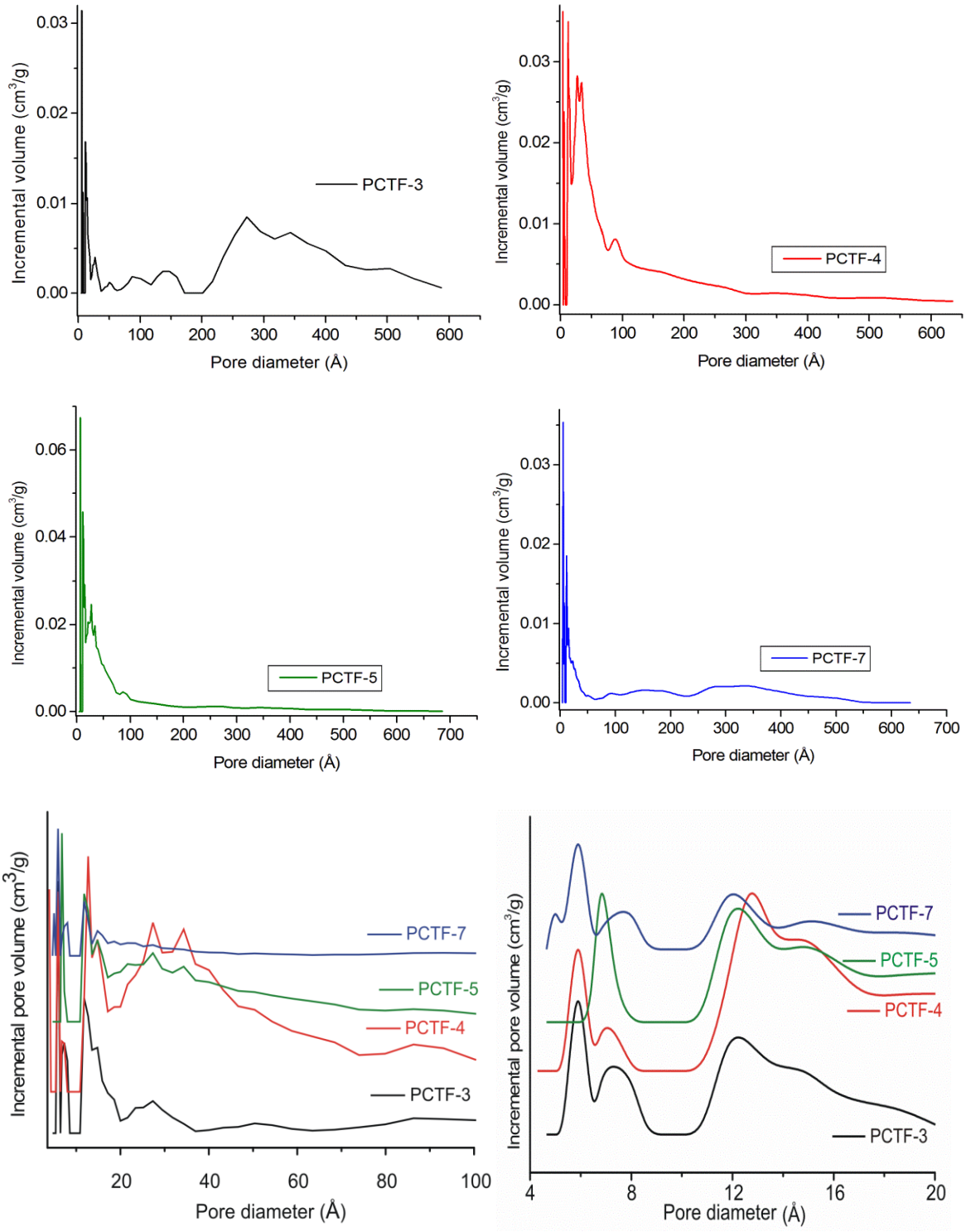

Fig. S7 Pore size distribution of PCTFs from N_2 adsorption isotherm (at 77 K) analysis.

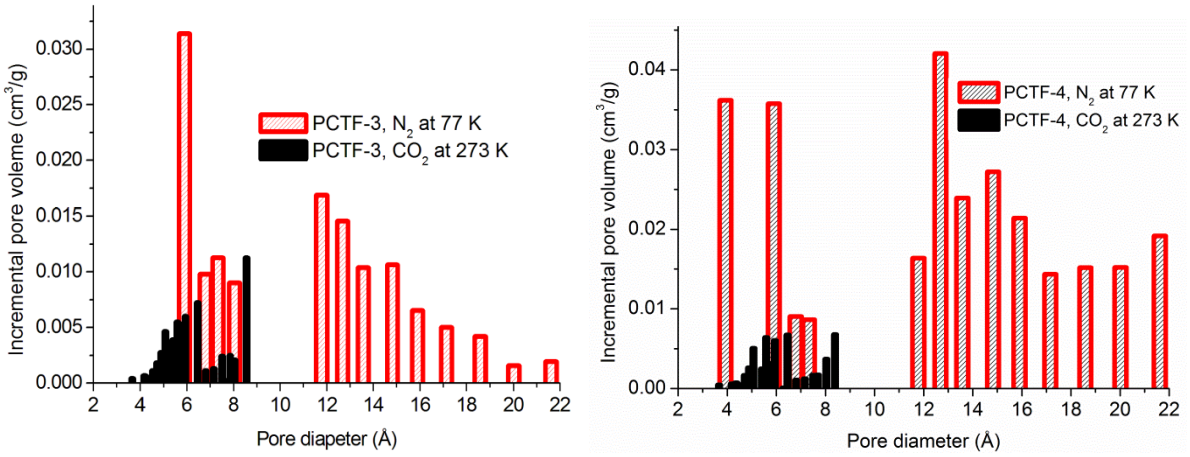

Fig. S8 Pore size distribution of PCTF-3 and PCTF-4 from analysis of N_2 and CO_2 adsorption isotherm.

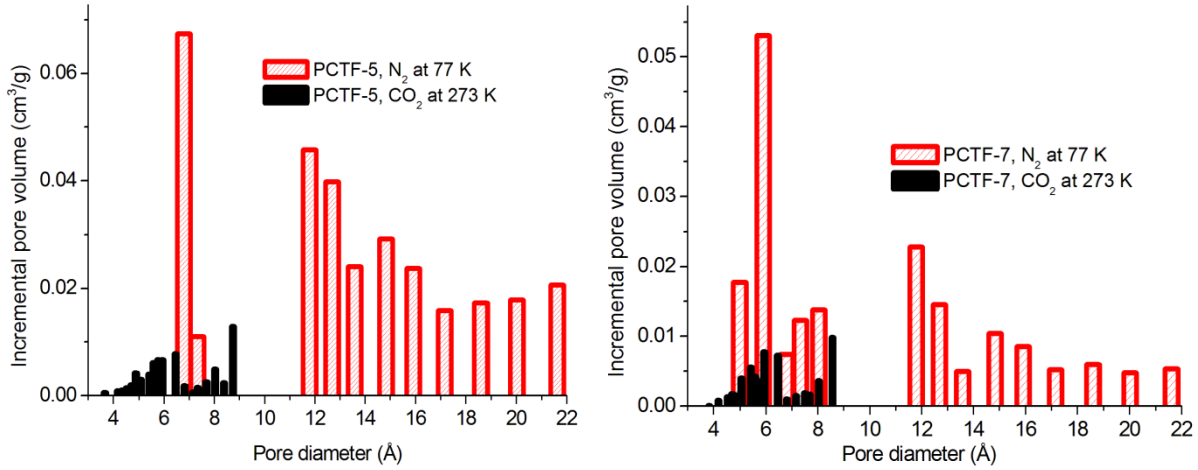

Fig. S9 Pore size distribution of PCTF-5 and PCTF-7 from analysis of N_2 and CO_2 adsorption isotherms.

7. Isosteric heats of adsorption of CO_2 for PCTFs

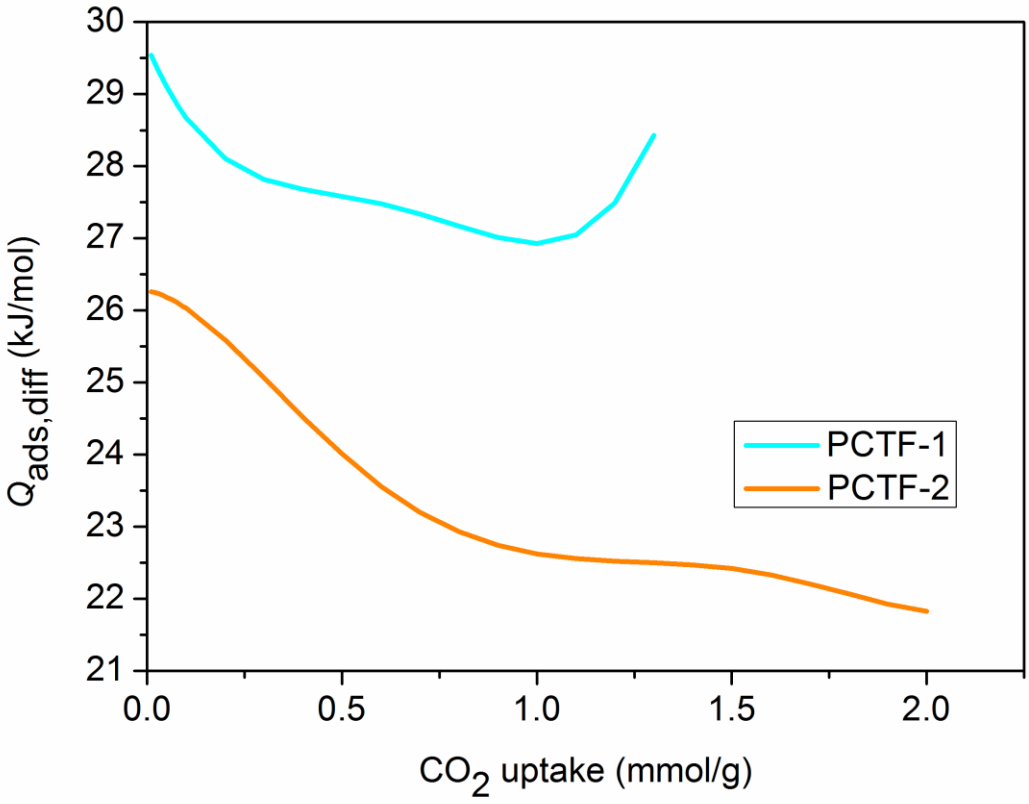

Fig. S10 Isosteric differential heat of adsorption (adsorption enthalpy, $Q_{ads,diff}$) as a function of CO_2 uptake for PCTF-1 to -2 (underlying adsorption isotherms were reported in ref. 4 and measured at 273 K and 293 K). In the thermodynamic context, the term *isosteric* denotes a process which occurs at a constant adsorbate loading, i.e., without ad- or desorption.

8. Plots of gas uptake (H_2, CO_2 and CH_4) *versus* BET surface area, V_{tot} and $V_{0.1}$ from N_2 adsorption isotherm analysis

The numbers 1 to 7 in the following figures refer to PCTF-1 to PCTF-7, respectively (cf. Scheme 1 and Scheme 2).

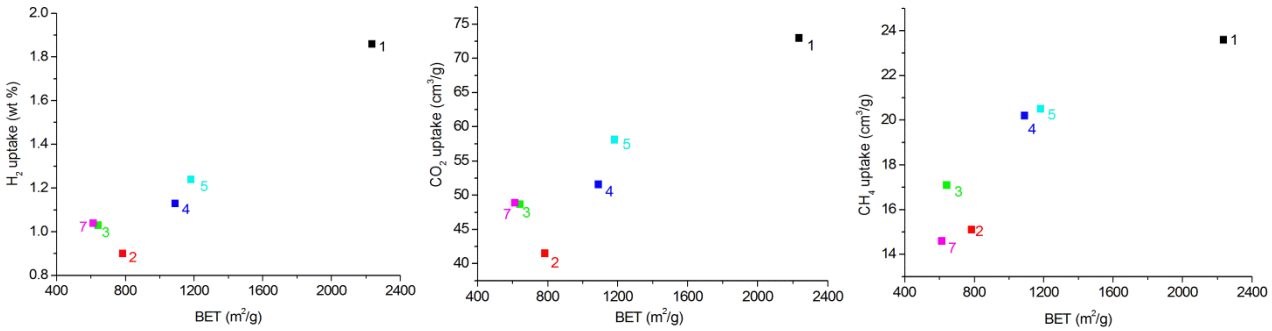

Fig. S11 Plot of gas uptake (from left to right: H_2, 77 K; CO_2, 273 K; CH_4, 273 K) *versus* BET surface area from N_2 (77 K) adsorption isotherm.

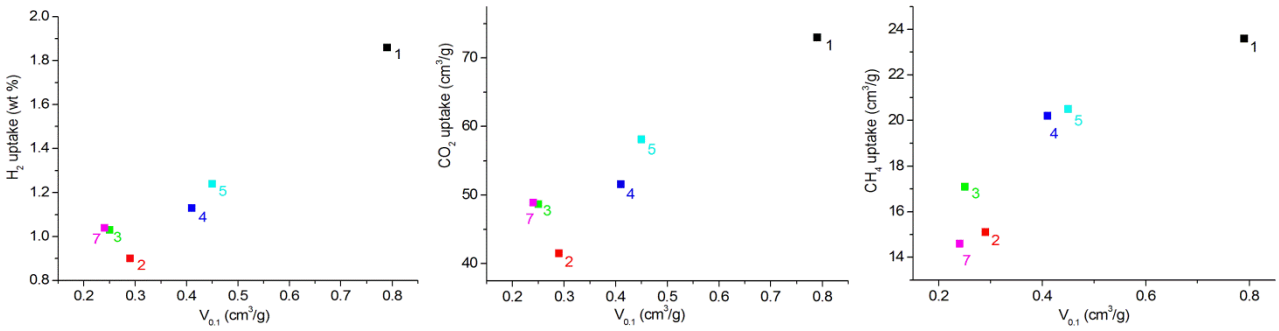

Fig. S12 Plot of gas uptake (from left to right: H_2, 77 K; CO_2, 273 K; CH_4, 273 K) *versus* micro pore volume ($V_{0.1}$) from N_2 (77 K) adsorption isotherm.

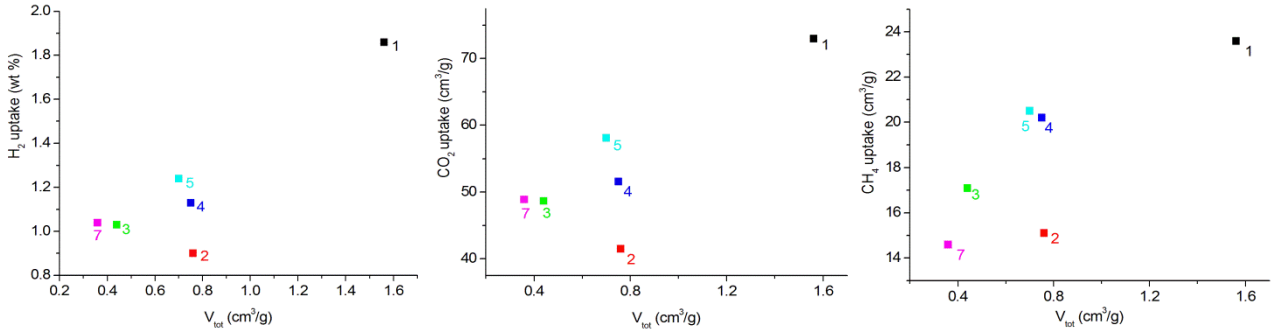

Fig. S13 Plot of gas uptake (from left to right: H_2, 77 K; CO_2, 273 K; CH_4, 273 K) *versus* total pore volume (V_{tot}) from N_2 (77 K) adsorption isotherm.

9. Gas selectivities

9a. from IAST method

TableS4 Toth parameters of gas adsorption isotherms and for IAST calculations at 273 K

	Toth parameters for gas adsorption isotherms			
Compound	Adsorptive	Max. adsorbed amount / mmol g^{-1}	Affinity constant b / kPa^{-1}	Toth constant t / -
PCTF-1	CO_2	19.22	0.00295	0.659
PCTF-2	CO_2	12.29	0.00426	0.486
PCTF-3	CO_2	6.77	0.01269	0.552
PCTF-4	CO_2	10.15	0.00867	0.489
PCTF-5	CO_2	12.19	0.00972	0.451
PCTF-7	CO_2	8.00	0.00993	0.534
PCTF-1	N_2	4.185	0.00099	0.805
PCTF-2	N_2	1.212	0.00316	1.287
PCTF-3	N_2	1.338	0.00251	0.956
PCTF-4	N_2	1.417	0.00233	0.913
PCTF-5	N_2	1.106	0.00326	1.379
PCTF-7	N_2	0.854	0.00225	0.947
PCTF-1	CH_4	8.89	0.00133	1.037
PCTF-2	CH_4	4.000	0.0028	0.684
PCTF-3	CH_4	2.105	0.00712	0.830
PCTF-4	CH_4	3.449	0.00427	0.818
PCTF-5	CH_4	3.990	0.00420	0.716
PCTF-7	CH_4	1.494	0.00715	1.064

TableS5 Henry constants ($H = max \cdot b$) for IAST calculations at 273 K

	H / mmol $(g\ kPa)^{-1}$ for adsorptive		
Compound	CO_2	N_2	CH_4
PCTF-1	0.05669	0.00414	0.01183
PCTF-2	0.05236	0.00383	0.01120
PCTF-3	0.08596	0.00336	0.01499
PCTF-4	0.08798	0.00329	0.01473
PCTF-5	0.11852	0.00361	0.01676
PCTF-7	0.07946	0.00192	0.01068

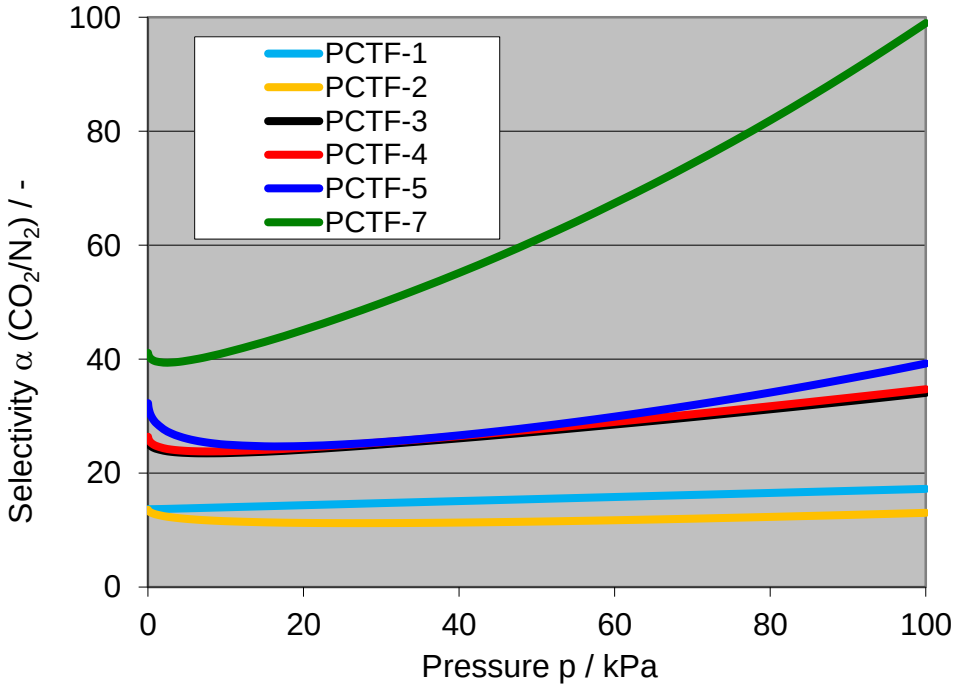

Fig. S14a IAST-predicted adsorption selectivity from an equimolar CO_2–N_2 gas mixture at 273 K for PCTFs.
Note that IAST calculations for PCTF-7 for the CO_2/N_2 selectivity are not very accurate because of the low N_2 loading of this compound.

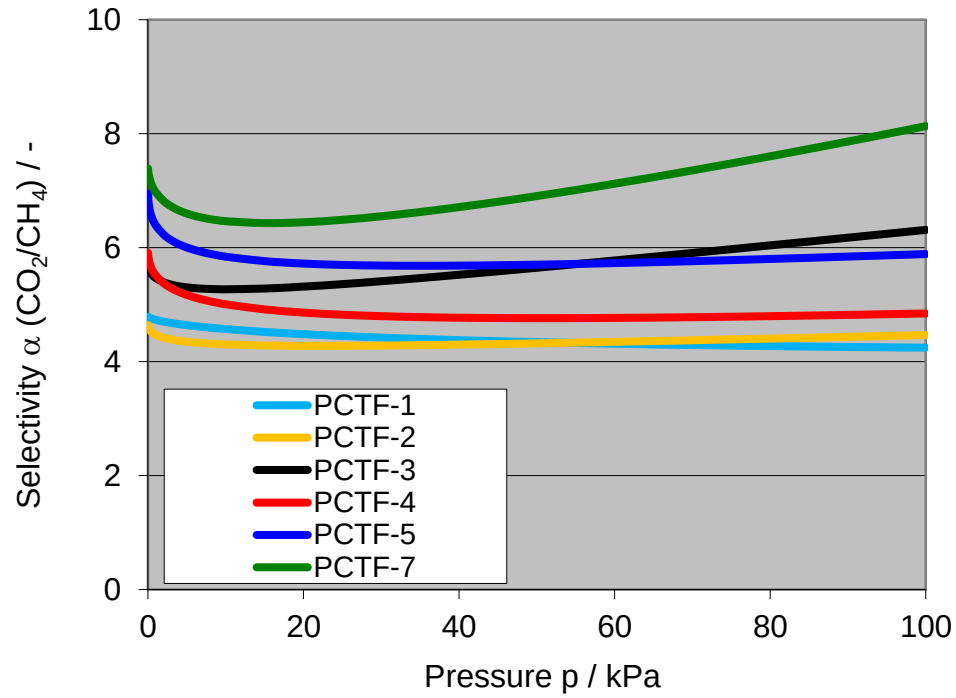

Fig. S14b IAST-predicted adsorption selectivity from an equimolar CO_2–CH_4 gas mixture at 273 K for PCTFs.

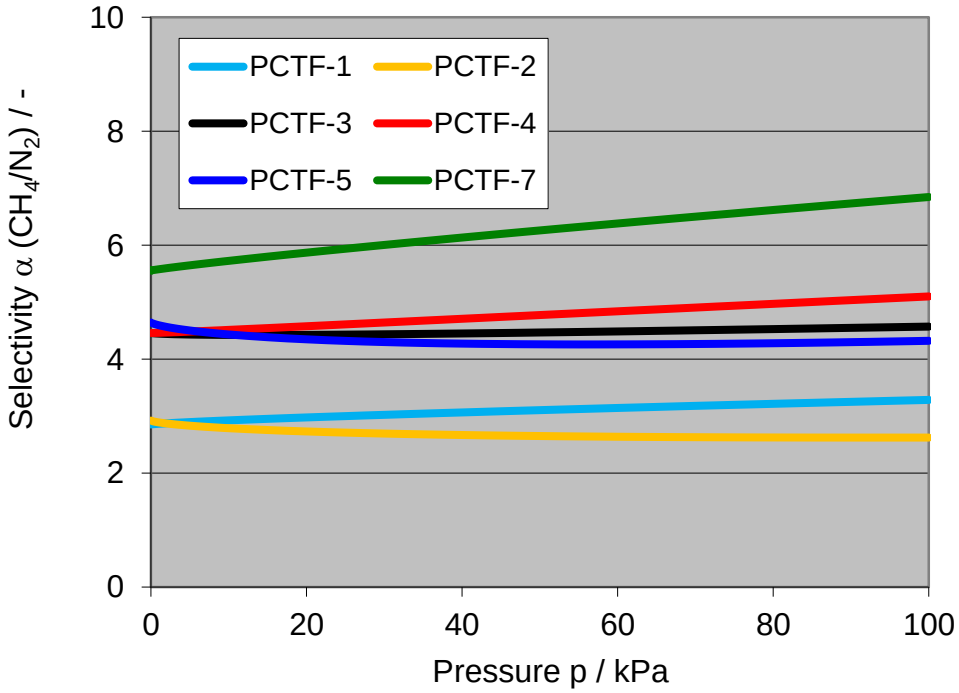

Fig. S14c IAST-predicted adsorption selectivity from an equimolar CH_4–N_2 gas mixture at 273 K for PCTFs.

9b. Gas selectivities based on initial slopes in the Henry region

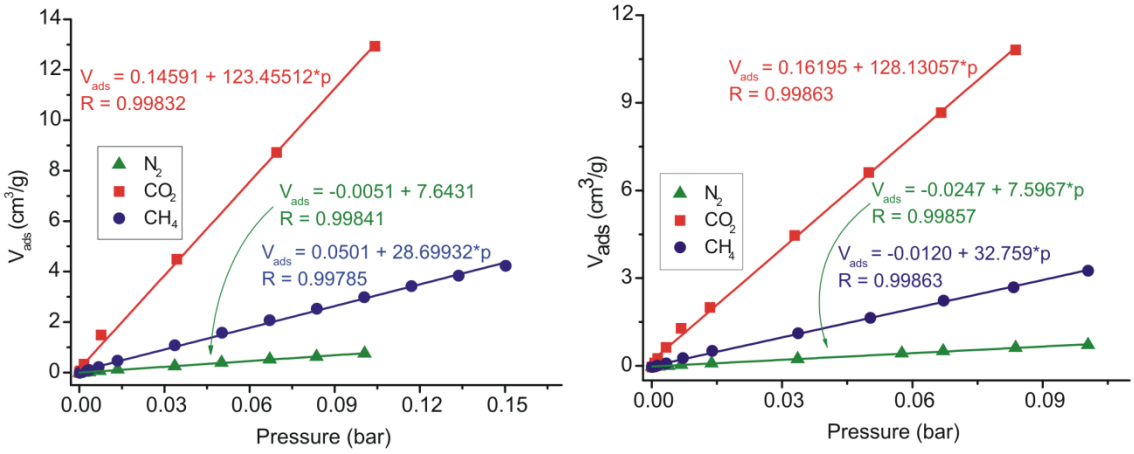

Fig. S15a The initial slopes in the Henry region of the adsorption isotherms for PCTF-3 (left) and PCTF-4 (right) at 273 K.

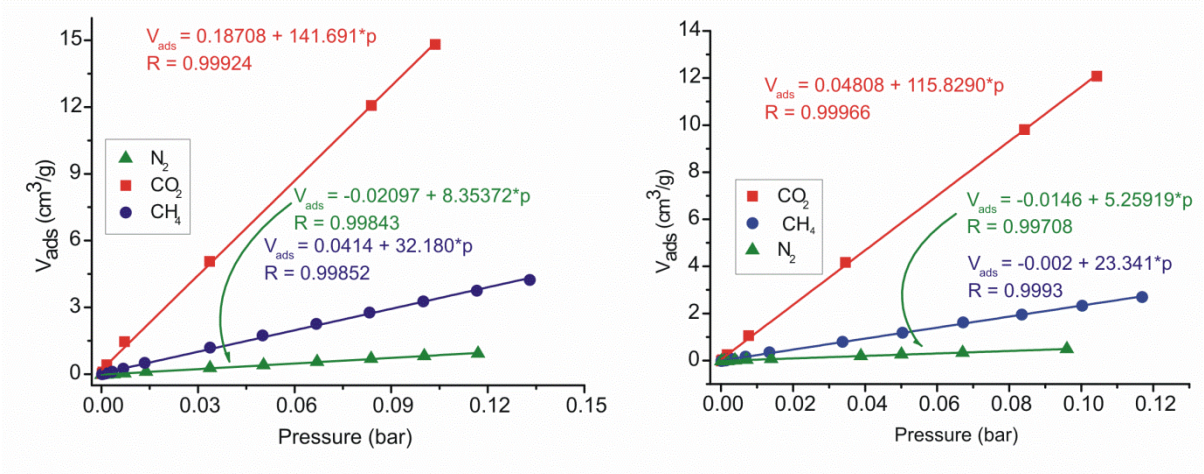

Fig. S15b The initial slope in the Henry region of the adsorption isotherms for PCTF-5 (left) and PCTF-7 (right) at 273 K.

Table S6 Initial slopes for gas adsorption isotherms and gas selectivities at 273 K

	Initial slopes for gas adsorption isotherms		
Compound	CO_2	N_2	CH_4
PCTF-3	123.5	7.6	28.7
PCTF-4	128.1	7.6	32.8
PCTF-5	141.7	8.3	32.2
PCTF-7	115.8	5.3	23.3
	Gas selectivities		
	CO_2:N_2	CO_2:CH_4	CH_4:N_2
PCTF-3	16:1	4:1	4:1
PCTF-4	17:1	4:1	4:1
PCTF-5	17:1	4:1	4:1
PCTF-7	22:1	5:1	4:1

10. References

1 V. R. Reichert and L. J. Mathias, *Macromolecules*, 1994, **27**, 7015-7023; H. Newman, *Synthesis*, 1972, 692-693.

2 I. Boldog, K. V. Domasevitch, I. A. Baburin, H. Ott, B. Gil-Hernandez, J. Sanchiz and C. Janiak, *CrystEngComm*, 2013, **15**, 1235-1243.

3 Y.-B. Men, J. Sun, Z.-T. Huang and Q.-Y. Zheng, *Angew. Chem. Int. Ed.*, 2009, **48**, 2873-2876.

4 A. Bhunia, V. Vasylyeva and C. Janiak, *Chem. Commun.*, 2013, **49**, 3961-3963.